AN EXPERIMENTAL STUDY ON INELASTIC BEHAVIOR AND RESTORING FORCE CHARACTERISTICS OF VIBRATION CONTROL DEVICE AS STEEL SCALING-FRAME

Shinichiro Tani [1] Seiya Shimada[1], Takumi Ito[2], DongHang Wu[3], Takashi Nagumo[4] and Haruhiko Hirata[5]

ABSTRACT

The innovated vibration control device called as scaling frame (abbreviated as "SF") structure is proposed by the author, DongHang Wu. SF structure consists of beam-column frame, diagonal bracing, and SF device installed. And vibration energy is absorbed by plastic behavior of diagonal deformation of SF. To investigate the inelastic behavior and restoring force characteristics of SF, the experimental examination of horizontally loading tests are conducted. Herein, the ratio of the size of SF to that of the beam-column frame is assumed with parameters as 8.5%, 10%, and 11.5%. From the test results, rigidity and strength of devices are inverse proportion to size of SF. And also, it is confirmed that the hysteresis behavior shows stable absorbed energy. Furthermore, the restoring force characteristics model of SF is proposed. From the comparison of test and analysis results, it can be said that the proposed model can chase the inelastic hysteresis behavior of test results accurately.

Keywords: steel structure, scaling frame, horizontal loading tests, restoring force characteristics

1. INTRODUCTION

Recently, a various type of vibration control device and damper has been developed, and most devices are adopted to actual building structure. For example, oil damper and high damping rubber device are suggested. They consist of special device and material, so there are some difficulties of getting material and technics. And, they have problems of durability and stability temperature and velocity. In contrast, SF structure can solve these difficulties, and provide transportability, workability and economy. SF structure consists of beam-column frame, diagonal bracing, and SF as shown in Figs.1, 2, and vibration energy is absorbed by plastic behavior of diagonal deformation of SF. SF structure has been used in wooden house already, and the effects of response mitigation and vibration control have been verified experimentally. Herein, to investigate the effectivity and applicability of SF on steel structures, the experimental examination of horizontally loading tests are conducted.

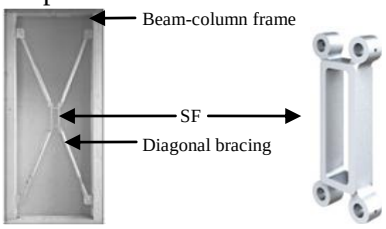

Fig.1 Scaling frame structure

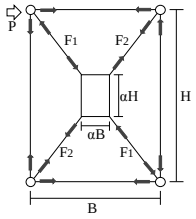

Fig.2 Concept of SF

2. GENERAL DESCTIPTION OF SF STRUCTURE

Herein, the general description of resistant mechanism and characteristics of SF structure is explained. The first, the relation of size of out-frame and SF is defined as reduction rate α as shown in Fig.2.

[1]Graduate Student, Tokyo University of Science, Tokyo, Japan, sinitiroutani1225@gmail.com,
[2]Associate Professor, Tokyo University of Science, Tokyo, Japan, t-ito@rs.kagu.tus.ac.jp
[3]President, Wu Building Office Corporation, Tokyo, Japan, wudonghang@wu-office.co.jp
[4]GM, Development Division, HORY Corporation, Tokyo, Japan, wt_nagumo@hory.jp
[5] Struc. Equipment. Sales Development, HORY Corporation, Tokyo, Japan, h_hirata@hory.jp

Figs.2 and 3 show the resistant mechanism of SF structure. From the principal of vertical work, the rigidity K_{sf}, yield strength P_y and plastic strength P_p are obtained as follows:

$$K_{SF} = \frac{24 \cdot E \cdot I_{SF} \cdot L^2}{\alpha^3 \cdot B^2 \cdot H^2 \cdot (B+H)} \quad (1)$$

$$P_y = \frac{4 \cdot f_b \cdot Z_{SF}}{\alpha \cdot H} \quad (2)$$

$$P_p = \frac{4 \cdot f_b \cdot Z_{psf}}{\alpha \cdot H} \quad (3)$$

Where E is the Young's modulus of the SF, I_{SF} is moment of inertia of area of the SF, Z_{SF} is elastic modulus of SF, Z_{pSF} is plastic modulus of SF, B is the length of the beam, H is the length of the column, L is the diagonal length of beam-column frame, and f_b is allowable bending stress of the SF.

From the above equations, it can be predicted that the rigidity is inverse proportion to a cube of reduction rate α, and the stress is inverse proportion to reduction rate α. Therefore, SF structure with small reduction ratio shows the large rigidity, strength and high energy absorption. However, in case of very small reduction rate of SF, the fracture would be occurred, so it is desirable that the limitation of reduction ratio is decided.

The next, the tensile and compressive deformation in the diagonal displacement of SF subjected to lateral force are dominated, it means that the diagonal bracing system is appeared. So the tensile and compressive displacements of each member are drawn in Fig.4 geometrically. From Fig.4, it can be said that the compressive displacement grows larger than the diagonal displacement of extension. Thus, the diagonal member on tensile side will resist increasingly, on the other hands, the diagonal member on compressive side will be reduced as shown in Fig.5. So the lateral buckling of diagonal member on compressive side is prevented.

This paper reports the loading test results, furthermore, this paper proposes restoring force characteristics model of SF that chase the inelastic hysteresis behavior of test results accurately.

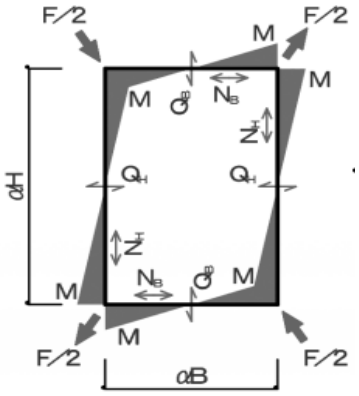

Fig.3 Diagram of bending stress of SF subjected to lateral force

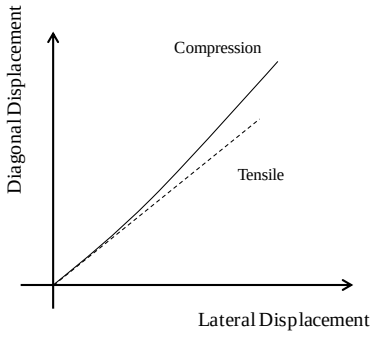

Fig.4 Comparison of compression and tensile deformation

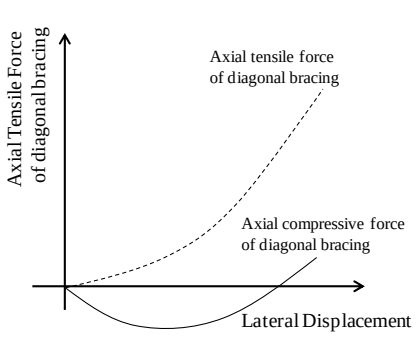

Fig.5 Relation of axial force and displacement

3. SUMMARY OF HORIZONTALLY LOADING TEST

3.1. General Description of Loading Test

This paper studies the inelastic behavior and restoring force characteristics of SF structure experimentally. Fig. 6 shows the test specimen of the SF. Herein, the reduction ratio of SF is considered with parameters as 8.5%, 10%, and 11.5%. Table 1 shows the size of the test specimens. The SF (thickness 19mm) is made of mild steel (JIS standard). Table 2 shows the mechanical properties of the steel used for the test specimen.

3.2. Test Set Up and Loading Test Methods

Fig.7 shows an elevation view of test set up. In this paper, the length of column is 1800mm, and that of beam is 1000mm. The SF connected with column jig through gusset plate and diagonal bracing. The loading jack is set on the beam jig. The horizontal force is measured from the load cell of the loading jack. The horizontal displacement at the top of the beam jig is measured by using a tape measure type displacement transducer, which is set as shown in Fig.7. The strain gauges are placed on the SF and the diagonal bracing as shown in Fig.8. During the loading tests, the maximum strain of the diagonal bracing remained 432μ (yield strain of the diagonal bracing is 1720μ). The loading program is arranged by the reference of the target displacement of the beam. The maximum angles of the column at each loop on the cyclic tests are 1/200, 1/100, 1/75, 1/50, and 1/30 (9mm, 18mm, 24mm, 36mm, and 60mm as the displacement of the beam). The maximum angle of the column is gradually increased, and the same two angles of the column for each cycle are repeated.

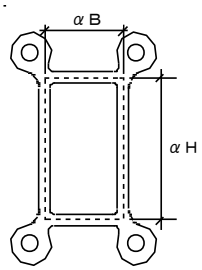

Fig.6 Layout of test specimen

Table1. Specimen sizes

Reducation rate	αB	αH
α-8.5	85	153
α-10	100	180
α-11.5	115	207

Table2. Mechanical properties of steel

Parts	Steel grades*	Yield strength(N/mm$^{2)}$	Tensil strength(N/mm^2)	Young's modulus(kN/mm^2)
SF	SS400	274	430	193
Brace(Web)	SS400	342	472	202

*Grade of JIS (Japanese Industrial Standards)

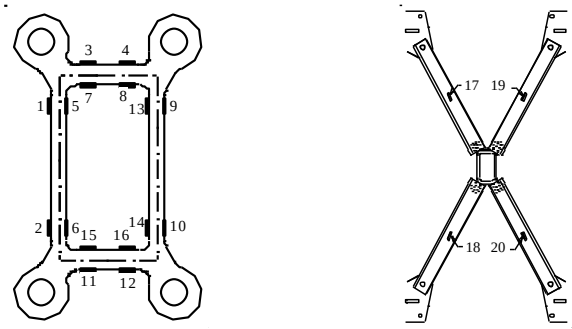

(a) SF (b) Diagonal bracing

Fig.8 Location of strain gauges

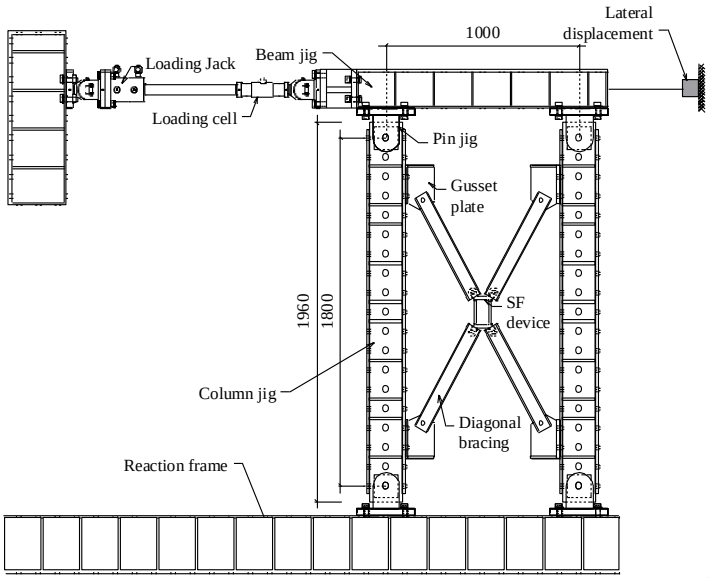

Fig.7 Elevation of test set up and location of sensors

(a) Test set up

(b) Deformation of SF before loading

Fig.9 Photographic of test set up

4. RESULTS OF TEST STUDY

4.1 Test Results of Monotonic Loading

Fig. 10 shows the relation of the lateral load P - displacement δ of the monotonic loading test results. And, Table 3 shows comparison of test results vs. calculation (Eqs.(1)-(3)). Herein, P_e is proportional limit strength, P_g is general yield strength.

From the test results of Fig. 10, it is confirmed that the rigidity and strength of the SF become large in case of small reduction rate α. And also, the strain hardening is appeared during ultimate state (around lateral displacement 60mm). From the analysis of axial and curvature of SF obtained from strain gauges, the curvature is dominated during early stage, however the axial deformation is advanced during ultimate states.

From the test results of Table 3, it can be said that P_y of theoretical value based on Eq.(2) shows almost similar with P_e of test result. So, the proportional limit strength P_e can be estimated by theoretical model considering the bending resistant mechanism.

Fig. 11 shows the relation of the axial force of diagonal bracing–lateral displacement. It is confirmed that the axial tensile force and axial compressive force of diagonal bracing are approximately equal in small deformation range. However, the axial compressive force decreases in large deformation range.

From the test result of Fig. 11(a), axial compressive force of diagonal bracing decreases, may turn tensile force soon as shown in Fig5.

4.2 Test Results of Cyclic Loading

Fig. 12 shows the relation of the lateral load P - lateral displacement δ of the cyclic loading test results. Also, Fig. 13 compares the skeleton curve obtained by monotonic loading test and envelope curve obtained by cyclic loading test.
In case of α-8.5, a little fracture around the corner of SF is observed at the angles of 1/30 rad. From the cyclic loading test results, the loop of the test results in case of all reduction rates shows almost same hysteresis and presents the stable behavior as shown in Fig. 12. In addition, the hysteresis behavior shows stable loop, it means that the SF absorbs the plastic energy in the small story drift angle. Furthermore, the skeleton curve corresponds approximately with the envelope curve as shown in Fig.13.

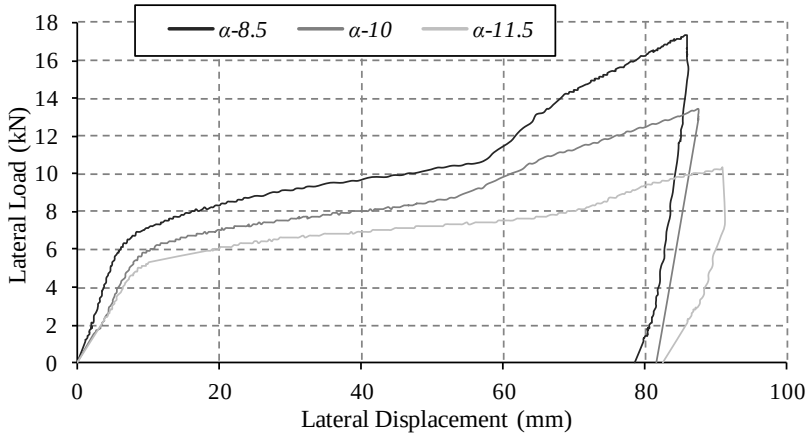

Figure 10 Monotonic loading test results of the SF

Table3. Comparison of test results and theoretical calculation

Reducation Rate	Yield Displacement[mm]			Yield Strength[kN]				
	expeimental value			expeimental value			theoretical value	
	μ=1600	δe	δg	μ=1600	Pe	Pg	Py	Pp
α-8.5	2.5	5.8	6.3	2.6	5.9	6.5	3.0	7.2
α-10	4.4	8.4	9.7	2.9	5.4	6.4	2.6	6.1
α-11.5	5.5	7.9	9.0	3.4	4.6	5.3	2.2	5.5

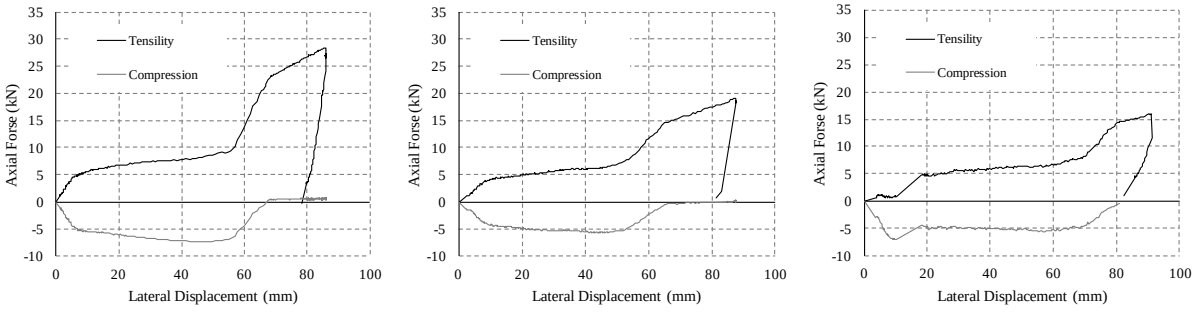

(a) α–8.5 (a) α–10 (a) α–11.5

Figure 11 Relation of axial force of diagonal bracing–lateral displacement curves

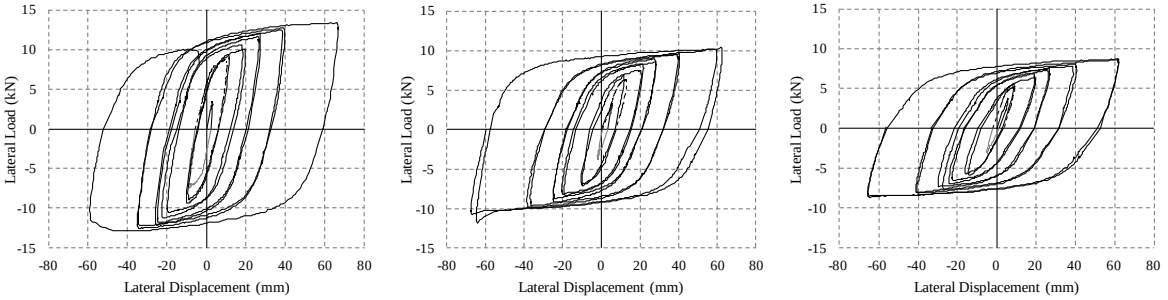

(a) α–8.5 (a) α–10 (a) α–11.5

Figure 12 Cyclic loading test results of the SF

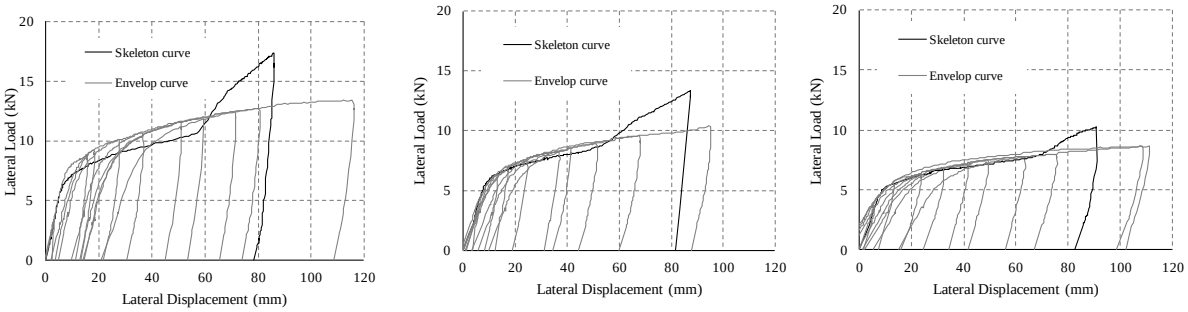

(a) α–8.5 (a) α–10 (a) α–11.5

Figure 13 Comparison of skeleton curves and envelop curves

5. PROPOSAL OF RESTORING FORCE CHARACTERISTICS MODEL

5.1 Skeleton Curve of Monotonic Loading

The skeleton curve of monotonic loading test results are approximated as tri-linear curve as shown in Fig. 14. Each break point of tri-linear curve is determined as follows; the first point is determined with the proportional limit strength, the second point is determined with general yield strength, and the third point is obtained from the test results.

5.2 Hysteresis Rule of Skeleton Shift Model

Herein, the cyclic hysteresis behavior is purchased with the skeleton shift model. “Skeleton Shift Model (Meng, Ohi and Takanashi, 1992)” was suggested to express strain hardening and stress softening behavior under inelastic cyclic loading. In this proposed model, an original form of the skeleton curve is composed of tri-linear curve and hysteresis loops are expressed by Ramberg-Osgood curve (Ramberg and Osgood, 1943). The summary of hysteresis rule is explained on Fig.15. In this paper, the shift coefficient and coefficient in Ranberg-Osgood function are adjusted by reference with test results.

5.3 Comparison of Test and Analysis Results

Fig.16 shows the comparisons of the hysteresis loops of the test results and analysis results. Herein, Fig.17 shows the relation of the accumulative displacement and the plastic absorbed energy. From the result of Fig. 16, it can be said that the proposed model can chase the inelastic hysteresis behavior of test results accurately. And also, from the result of Fig. 17, the absorbed plastic energy on the analysis corresponds to the test result.

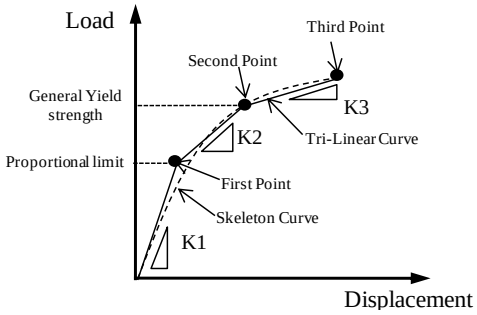

Figure 14 Definition of skeleton curve

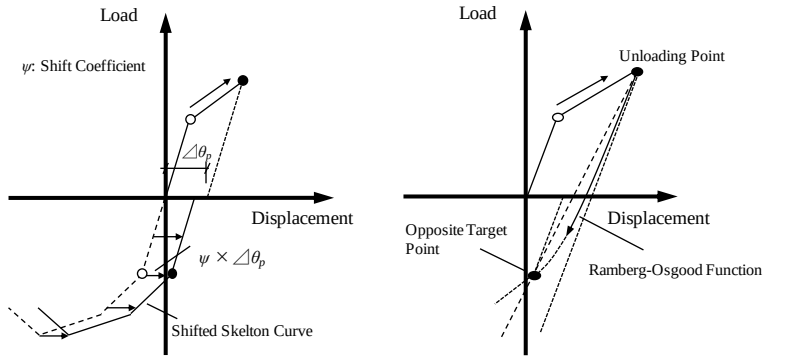

(a) Shifted skeleton curve (b) Ramberg-Osgood curve

Figure 15 Hysteresis rule of the Skeleton Shift Model

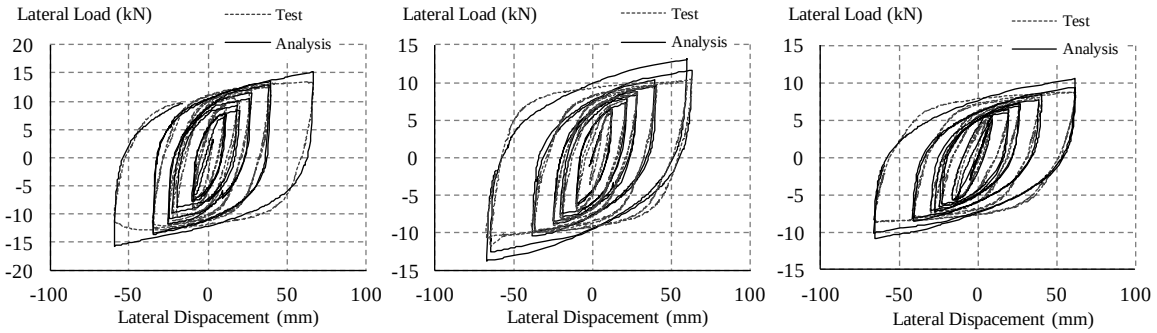

(a) α–8.5 (a) α–10 (a) α–11.5

Figure 16 Comparison of test and analysis results

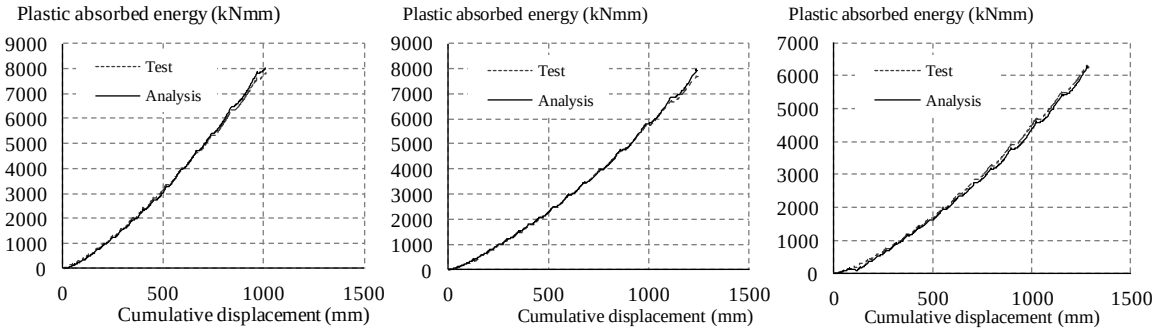

(a) α–8.5 (a) α–10 (a) α–11.5

Figure 17 Relation of cumulative displacement and plastic absorbed energy

6. CONCLUSIONS

This paper proposed the innovated vibration control device called as scaling frame, and investigated the inelastic behavior and restoring force characteristics of SF by experimental examination of horizontally loading tests. The remarkable conclusions of this paper are as follows:

1. The SF with small reduction ratio α can provide the large rigidity and strength.
2. From the comparison of strength of test results, the theoretical model abstracted from principal of vertical work can predict the strength of test results well.
3. The resistant mechanism of SF is divided as follows; the bending mechanism such as moment resisting frame, and axial force mechanism.
4. The compressive force generated in diagonal member decreases as lateral deformation increases. It means that the lateral buckling is prevented geometrically.
5. The hysteresis behavior shows stable, and it can absorb the plastic energy.
6. The hysteresis model during cyclic loading is presented with Skeleton Shift Model, and it shows good agreements with test results.

ACKNOWLEDGMENTS

This research was supported by Grant-in-Aid for Scientific Research (C) (Head : Takumi Ito).

REFERENCES

Meng L. Ohi, K,, and Takanashi,K.(1992). “A simplified model of steel structural members with strength deterioration used for earthquake response analysis”. *Journal of structural and construction engineering*. **No437**, 115-124

Ramberg, W. and Osgood,W. R. (1943). “Description of stress –strain curves by three parameters.” *National Advisory Committee on Aeronautics*. **Technical Note 902**.